SEMARAK ILMU PUBLISHING

CFD Letters

Journal homepage:
https://semarakilmu.com.my/journals/index.php/CFD_Letters/index
ISSN: 2180-1363

CFD Analysis on Different Filling Volume Capacity and Fluid Density for Flexitank Application

Mohamad Amirur Rahman Azahar[1], Nofrizalidris Darlis[2,*], Norhafizzah Hassan[1], Zuliazura Mohd Salleh[3], Syafiqah Ruqaiyah Saiful Azam[1], Ishkrizat Taib[4], Mohd Zamani Ngali[4], Khairul Nizam Mustaffa[5], Muhamad Mohshein Hashim[5]

[1] Department of Mechanical Engineering Technology, Faculty of Engineering Technology, Universiti Tun Hussein Onn Malaysia, Pagoh, Johor, Malaysia
[2] Centre of Automotive and Powertrain Technology, Faculty of Engineering Technology, Universiti Tun Hussein Onn Malaysia, Pagoh, Johor, Malaysia
[3] Integrated Engineering Simulation and Design, Faculty of Engineering Technology, Universiti Tun Hussein Onn Malaysia, Pagoh, Johor, Malaysia
[4] Faculty of Mechanical and Manufacturing Engineering, Universiti Tun Hussein Onn Malaysia, Batu Pahat, Johor, Malaysia
[5] My Flexitank Industries Sdn Bhd, Plot 3&4, Jalan PKNK 3, Kawasan Perindustrian LPK Fasa 3, 08000 Sungai Petani, Kedah, Malaysia

ARTICLE INFO

Article history:
Received 11 August 2022
Received in revised form 20 September 2022
Accepted 28 November 2022
Available online 12 January 2023

Keywords:
Bulk Liquid; Transportation; Sloshing; Computational Fluid Dynamics (CFD); Fluid-Structure Interaction (FSI); Flexitank; Hydrodynamics

ABSTRACT

When it comes to the structural design of flexitanks used for freight transportation, liquid sloshing is a crucial subject of concern. However, with consideration of the flexitank shape, there is no specific capacity value that can be used as a guide for filling the liquid inside it. This phenomenon may cause a high-pressure impact on the flexitank, resulting in a leakage on the LLDPE package. One of the solutions to reduce the frequency of leaks occurred is to fill up the acceptable volume based on hydrodynamics performance. Therefore, the purpose of this paper is to investigate, using commercial computational fluid dynamics (CFD) software, the hydrodynamic performance of various flexitank filling volume capacities based on different liquid densities. This is evaluated by comparing the hydrodynamics study for filling capacities that are 1%, 2%, and 3% higher than the rated capacity for flexitanks that has been suggested by the Container Owner Association (COA). Due to the flexitanks thin walls, it is important to consider the impacts of fluid-structure interaction (FSI). To do this, a partitioned FSI approach is used by coupling the CFD and FEA solvers for this multi-physics issue. The main standpoint of FSI is that fluid forces are applied to structures, causing deformation. Hydrodynamic parameters such as structural deformation on flexitank, von-mises stress and von-mises strain were used to identify the suitable filling capacity for three different: water, latex, and crude palm oil, as these liquids are commonly used for flexitank. The results indicate that varying the liquid filling capacity affected the hydrodynamic performance of the flexitank. Following that, increasing the flexitank filled with water by 3% and increasing the flexitank filled with latex and CPO by 1% can lead to structural damage as it gives highest maximum value of total deformation for these capacities. Since the situation of the flexitank are in the braking condition, the highest elastic equivalent strain is occurred at the front-top of the flexitank structure.

**Corresponding author.*
E-mail address: nofrizal@uthm.edu.my

https://doi.org/10.37934/cfdl.15.1.115126

1. Introduction

Transportation is the most important role in supply chain operations, as it follows for the movement of goods from the place where it was initially manufactured to the place where it ultimately demanded [1]. In addition, the efficiency of the chosen mode of transportation is extremely important because it is directly related to the cost-effective success of the supply chain [2].

Bulk liquid transport is one of the most important modes of fluid package transport, whether by sea or land. Instead of using drums or tanks, it entails shipping the bulk liquid in a tanker truck. So then, the tank can be transported in the same way as any other truckload of freight. The concept of liquid transport has many different aspects that need to be taken under consideration. These liquid cargoes, which include chemicals, liquefied natural gas, and crude oil, are not manually stored or packaged. Despite this, they are put into and sucked out of a Parcel Tanker's huge tank areas, referred to as the holds. Bulk liquids can be transported in a variety of ways, including standard International Standardization Organization (ISO) containers and plastic flexicontainers, by means of a variety of various trailers. However, bulk tankers are the most used container for transporting liquids, both edible and inedible.

The basic problem concerning liquid sloshing is the estimation of the hydrodynamic pressure distribution, forces, moments, and natural frequencies of the free-liquid surface. These factors have a direct impact on the dynamic stability and performance of moving containers. When the frequency of the tank motion is near to one of the inherent frequencies of the tank fluid, large sloshing amplitudes might be expected [3]. The sloshing phenomena has drawn more interest in recent times, and several research utilizing various methods have been carried out.

Sloshing has been studied by numerical methods such as the finite element method (FEM) [4-6], the computational fluid dynamics (CFD) method [7–11], or the smoothed particle hydrodynamics (SPH) method [12-13]. For most practical problems, the sloshing is determined by both the tank properties and the motion of the vehicle carrying it. For example, the coupled SPH-FEM has been studied by Camas *et al*., [14] and coupled BEM-CFD by Saripilli *et al*., [15]. Additionally, the fluid-structure interaction (FSI) has been widely utilized to analyse the effects of sloshing on the tank structure. The coupling strategy between CFD and finite element analysis (FEA) has been studied by Arora *et al*., to analyze the sloshing-induced loads on a fuel tank structure [16]. Finally, The FSI approach was utilised by Ganuga *et al*., [17] to examine the internal structure of a sloshing tank that is sensitive to resonance.

Therefore, this paper aims to analyze the hydrodynamics performance on different flexitank filling volume capacity and fluid density using one-way coupling of FSI strategy by coupling the CFD and FEA solvers. Previous study suggests that CFD analysis can be utilized to conduct a detailed hydrodynamics study on the sloshing of the flexitank container, which is the best technique for observing and analyzing the sloshing effect. In addition, the flow simulation can investigate the sloshing phenomenon and its associated hydrodynamics, such as the turbulence flow in the flexitank.

2. Methodology

2.1 Geometry Modelling

The size of the flexitanks used in this study are according to the specifications given by MY Flexitank Industries Sdn Bhd [16]. Computer-Aided Design (CAD) software, SolidWorks was used to create all the flexitank geometry, and CFD software, Ansys was used to run the simulation. Figure 1 shows the geometry drawing of flexitank. The size of the flexitanks used in the simulation, such as

the capacity, length, width, and height are shown in Table 1. According to Container Owner Association (COA), the guidelines for flexitank loading used is not more or less than 500 liters of the flexitank rated capacity [18]. Hence, the capacity of liquid used in this study was set for 1%, 2%, and 3% more than reference capacity.

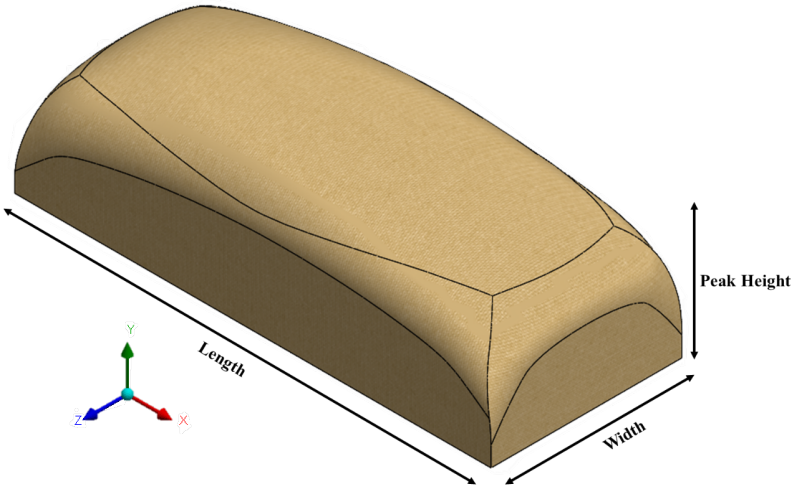

Fig. 1. Flexitank geometry modelled in SolidWorks

Table 1
Details of flexitank sizes

Flexitank size	Capacity (L)	Length x Width (mm)	Peak Height (mm)
Reference	21,000	3,028 x 2,362	2,223
+ 1%	21,210	3,028 x 2,362	2,244
+ 2%	21,420	3,028 x 2,362	2,255
+ 3%	21,630	3,028 x 2,362	2,264

2.2 Fluid Properties

The physical properties of fluids are critical for predicting their hydrodynamics performance in flexitank. The simulated properties were referred based on few research studies. According to MY Flexitank Industries Sdn Bhd, latex and CPO are the main products used by most of their customers. Thus, the latex and crude palm oil (CPO) was chosen to add variants in different base fluid studies. Table 2 shows the physical characteristics of the fluid utilized in the study.

Table 2
Physical properties of the fluids used in the current study

Fluid	Density, ρ(kg/$m3$)	Viscosity, μ (kg/m. s)	Reference
Water	997	0.001	[19]
Latex	950	0.042	[20]
CPO	890	0.077	[21]

2.3 Mechanical Properties of Flexitank Structure

The flexitank have been made from various materials by different manufacturers around the world. The material used in this study is Low-Linear Density Polyethylene (LLDPE), which is used by the company. LLDPE is a type of polyethylene that is commonly used for packaging due to properties

such as low shear sensitivity, ease of processing, and greater fluidity. Table 3 shows the physical and mechanical properties of LLDPE.

Table 3
LLDPE properties [22]

Physical Properties	Unit	Tolerance ±	Value	Testing Method
Thickness	mil	2	12	Thickness gauge
Density	Kg/m^3	-	920	ASTM D-1505
Mechanical Properties	**Unit**	**Tolerance ±**	**Value**	**Testing Method**
Tensile strength MD	MPa		29.2	
Tensile strength TD			14.1	
Break elongation MD	%	10	245	ASTM D-882
Break elongation TD			540	
Dart drop	g		40	ASTM D-1709
Puncture	kg		1.7	
Stretching level	-	-	110	High-light tester

2.4 Mesh generation

Meshing is an important stage before numerical simulation to divide the complex geometries into more simple elements to use as local approximation. If the meshing produces an excessive number of cells, the computational time will be prolonged and inefficient. If the meshing produces too few cells, the simulation results for the study will be inaccurate. Therefore, the meshing method is significant and will affect the accuracy, convergence, and speed of simulation.

The geometry of the flexitank is meshed in Ansys advanced meshing module. In this study, the mesh is divided by two domain which is fluid domain and solid domain. Figure 2(a) illustrates how the mesh is formed at the fluid domain while Figure 3(b) shows the mesh result at the solid domain. The tetrahedron approach was used to mesh the model due to its simplicity. Automatic mesh generation is used for global meshes, whereas manual mesh generation is used for local meshes.

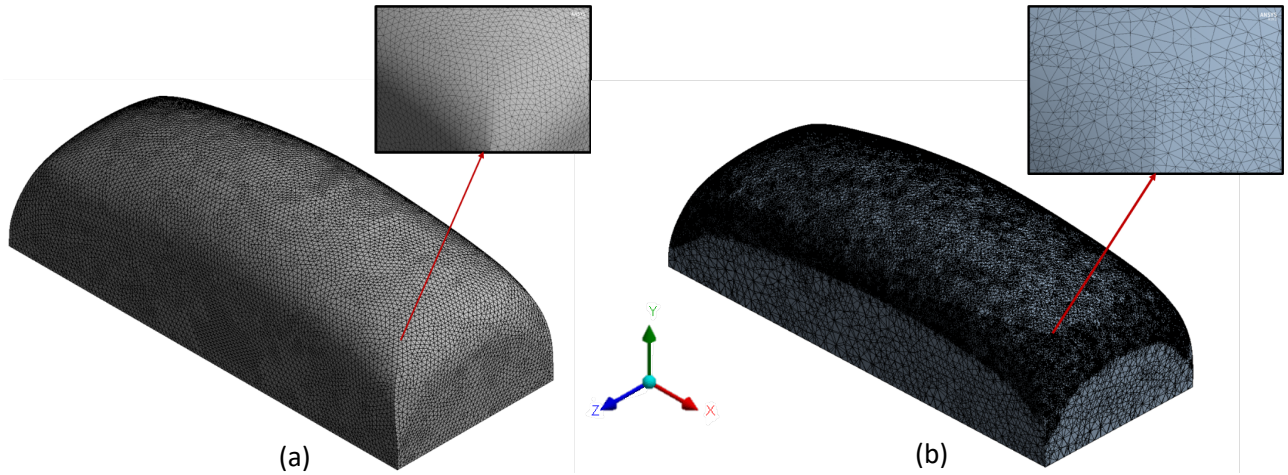

Fig. 2. Mesh development for the following domains: (a) fluid (b) solid

2.3 Numerical Procedure

2.3.1 Simulation setup and boundary conditions

In this study, flexitank was simulated using Ansys CFD software to analyse hydrodynamic performance for various filling volume capacities. A SIMPLE discretization of pressure-velocity coupling is chosen, which makes equation convergence difficult but increases solution precision. The scalable wall function and k- ω SST turbulence model is implemented.

Near the wall region, where an adverse pressure gradient forms, the k- ω SST turbulence model can solve turbulence parameters [23]. Via Ansys software, fluid flow and transient structural simulations are coupled to develop the fluid-structure interaction model. These two solutions are coupled to provide an FSI interface between the fluid domain and the structural domain.

Figure 3 illustrates the computational domain used in this study. At the fluid domain, the outer face of the model is considered as fluid wall. The fixed support of the model was represented by the face that fully meets with the container body. Meanwhile, the outer wall of the solid domain is considered as the fluid solid interface where the imported pressure from fluid domain is attached.

The velocity profile used in this study are according to the driving cycle studied by N. N. Clark et. al., [24]. Due to computational limitation, the data is only taken while in braking condition where in the last 6 seconds, the velocity decreases from 4.4 m/s (16 km/h) to 0 m/s. Table 4 shows the summary of boundary conditions used in this study.

Table 4
Boundary conditions

Type of tank	Capacity (L)	Velocity (m/s)	Turbulence model	Type of flow
Flexitank	21,000 + 1,2,3 %	4.4 – 0 (Braking)	k–ω SST	Transient state

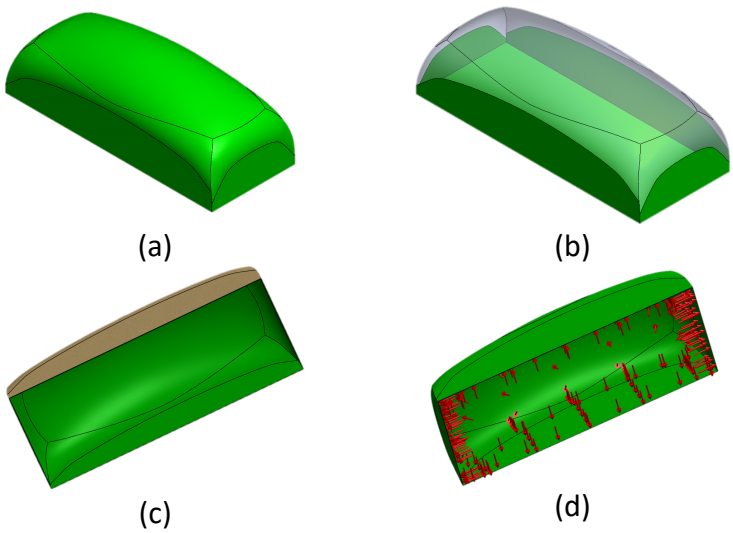

Fig. 3. The boundary conditions for (a) fluid wall (b) fixed support (c) fluid solid interface (d) imported pressure from fluid domain

2.3.2 Governing equation

2.3.2.1 The standalone CFD model

The flexitank is excited sinusoidally along the length of the flexitank (x-direction) given by

$$x = A\sin(\omega t) \tag{1}$$

where x is the displacement, A is the amplitude of excitation and ω is the angular frequency of the oscillation. The acceleration $\ddot{x}$ corresponding to the displacement Eq. (1) is given by

$$\ddot{x} = -A\omega^2 \sin(\omega t) \tag{2}$$

It is assumed that the liquid and the gas phases are incompressible [25-26]. The cavitation and thermal effects are neglected. The no-slip condition (velocity of the liquid at the flexitank walls is equal to the velocity of the tank) was taken as the boundary condition on all the flexitank walls. Finally, the governing equations associated with sloshing that are solved, are the continuity Eq. (3) and the momentum conversation Eq. (4) for an incompressible flow is given by

$$\nabla \cdot u = 0 \tag{3}$$

$$\frac{\partial \boldsymbol{u}}{\partial t} + (\boldsymbol{u}\cdot\nabla\boldsymbol{u}) = -\frac{\nabla p}{\rho} + \vartheta\nabla^2\boldsymbol{u} + \sigma\kappa\boldsymbol{n} + \boldsymbol{g} + \ddot{\boldsymbol{x}} \tag{4}$$

Volume of Fluid (VOF) method [27] for tracking the free surface of the liquid is given by

$$\frac{\partial \alpha}{\partial t} + \nabla\cdot(\alpha\boldsymbol{u}) = 0 \tag{5}$$

In the above equations u is the fluid velocity, p is the fluid pressure, ρ is the fluid density, ϑ is the kinematic viscosity of the fluid, σ is the surface tension coefficient between fluids, surface tension causes a force that moves in the direction that is normal to the interface n = ∇α/|∇α|, α is the volume fraction, κ is the local curvature to the interface, g is the gravity, and t represents time [28].

2.3.2.2 The fluid-structure interaction modelling

The behavior of the structure in response to fluid motion is determined by the two conservation principles of mass Eq. (6) and momentum Eq. (7):

$$\nabla u^s = 0 \tag{6}$$

$$\rho^s\left(\frac{d^2\boldsymbol{y}}{dt^2} + \eta\frac{d\boldsymbol{y}}{dt} - \boldsymbol{f}^s\right) - \nabla\cdot\boldsymbol{\sigma}^s = 0 \tag{7}$$

where superscript s indicates the structure, u, ρ, y, η, f, and σ are the velocity, material density, structural displacement, damping coefficient, external force, and Cauchy stress tensor respectively. The boundary condition for the structural analysis is that the bottom wall is fixed at the four corners of the container. Therefore, at the fixed points, the structural and angular displacements are given by

$$\gamma = 0 \tag{8}$$

$$\theta = 0 \tag{9}$$

where θ refers to angular displacement.

3. Result

2.1 Grid Independence Test

Grid independence is a phrase used to explain how utilizing successively smaller cell sizes for the computations improves the results. The phrase "grid independence" refers to the idea that a calculation should tend toward similar outcomes when the mesh size is reduced. Figure 4 depicts the velocity for one of the flexitank models which is 21,000 L with a different number of nodes. As a result, the mesh's size was approximately increased from 253 K to 492 K nodes to see the significant changes in velocity. According to the grid independence test, the velocity distribution has not significantly changed from the node of 347 K to the node of 492 K, with an average relative error of less than 1%. As a result, the subsequent simulations are set to include 347 K nodes or more. The cell size should be gradually decreased when this model approaches grid independence to reduce error caused on by discretization and to use the same mesh configuration as the other models.

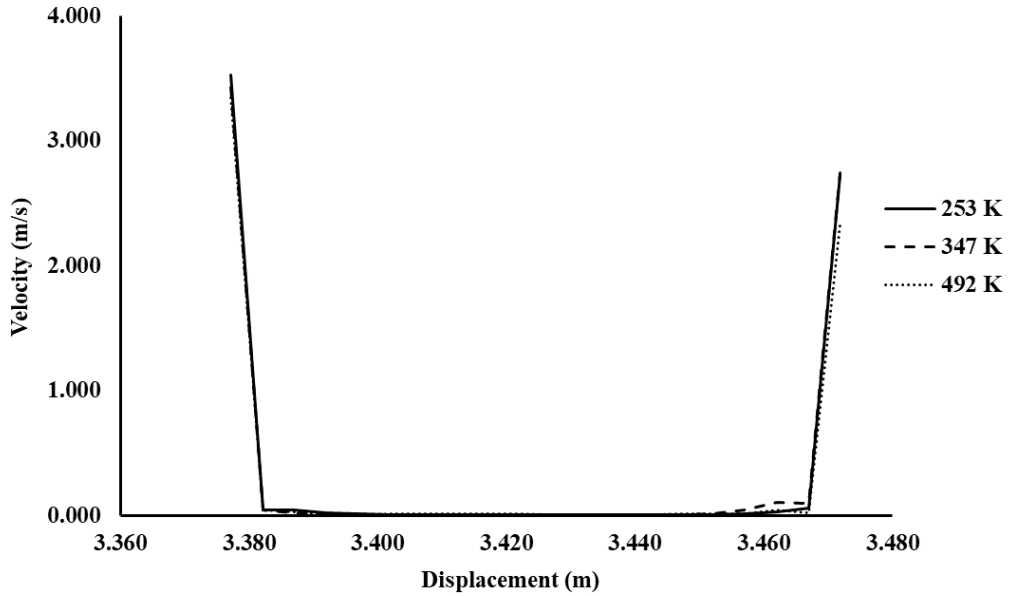

Fig. 4. Grid independence test result for three different nodes number

3.2 Total Deformation on Flexitank Structure

Deformation in physics is the change of a body using continuum mechanics from one configuration to another [29]. A configuration is a set of all the locations of a body's constituent components. External loads [30], intrinsic activity (like muscle contraction), body forces (such gravity or electromagnetic forces), changes in temperature, moisture content, or chemical reactions are all possible causes of deformation.

Table 4 shows the contour of total deformation occurred at top surface of flexitank structure that has been filled with water, latex, and CPO for different filling volume capacity. As the flexitank is used to be filled with 21,630 L of water, some deformation appears on the top-side of the structure,

demonstrating that 21,630 L flexitank has the larger deformation compared to other capacities. By comparing with the reference capacity, increasing the water inside flexitank by 3% will increase the maximum number of total deformations by 81%. However, for the cases of latex and CPO that have low density compared to water, it gives different situation when increasing the fluid capacity by 1% will resulted the highest deformation on both flexitank structure. It clearly can be seen in the Table 4 where the red color of contour is mostly occurred at 21,20 L flexitank. Furthermore, total deformation for the flexitank filled with latex and CPO is slightly different when the flexitank is filled with increased capacity of 2% and 3%.

It can be concluded that increasing the flexitank filled with water by 3% and increasing the flexitank filled with latex and CPO by 1% can lead to structural damage as it gives highest maximum value of total deformation for these capacities as shown in Figure 4.

Table 4
Total deformation on flexitank structure

Fluid	21,000 L	21,210 L	21,420 L	21,630 L
Water	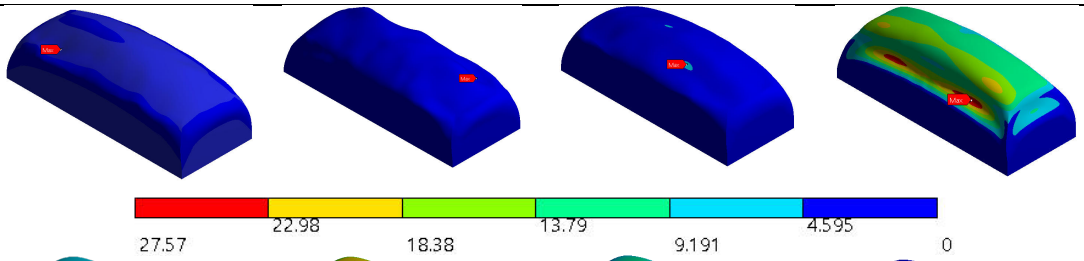			
Latex	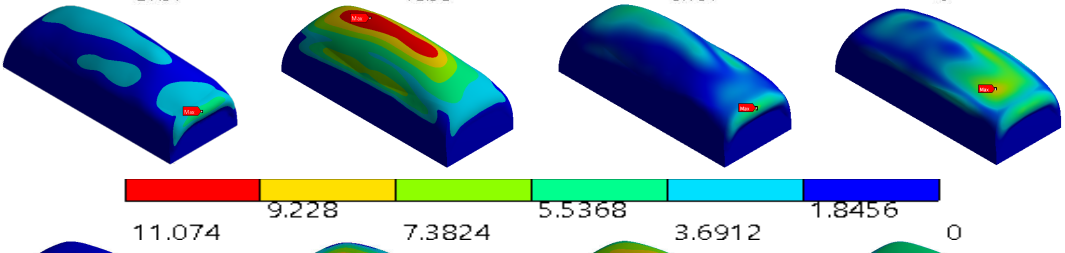			
CPO	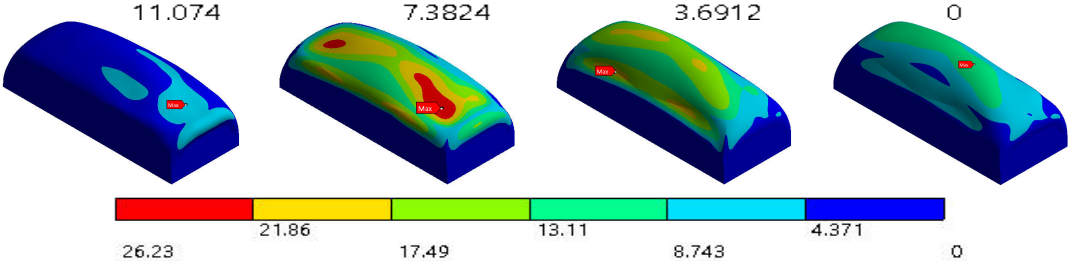			

3.3 Von-mises Stress

A value defined as the von-mises stress is used to determine whether a certain material may yield or fracture. According to the von-mises yield criteria, a material will yield if its von-mises stress under load is equal to or greater than its yield limit under simple tension.

Table 5 shows the contour of von-mises stress, and the position of maximum stress occurred for different filling volume capacity of flexitank filled with water, latex, and CPO. For the flexitank with water, the largest equivalent stress, which is 5.698 mm occurred at 21,630 L flexitank, meanwhile the lowest equivalent stress occurred at 21,210 L flexitank with the value 0.092 mm. It also shows that increasing the flexitank filling volume filled with latex will reduced the maximum equivalent stress where all these flexitank has lower equivalent stress than reference capacity. According to the

same table, it shows the 21,210 L flexitank filled with CPO has the largest equivalent stress which is 5.397 mm while the reference flexitank has the lowest equivalent stress with the value of 3.955 mm.

For the water, it shows that increasing the filling volume by 1% will reduced the equivalent stress on flexitank structure by 65%. In addition, increasing the filling volume for latex by 3% will also reduce the equivalent stress by 32%. However, increasing the filling volume for CPO will increase the equivalent stress by 10% – 36%.

Table 5
Von-mises stress on flexitank structure

Fluid	21,000 L	21,210 L	21,420 L	21,630 L
Water	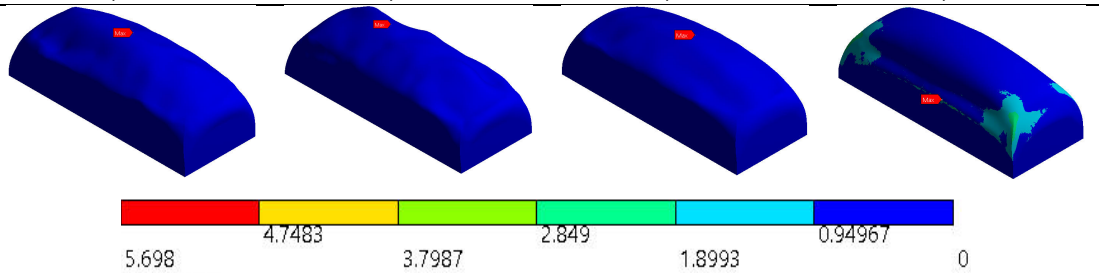			
Latex	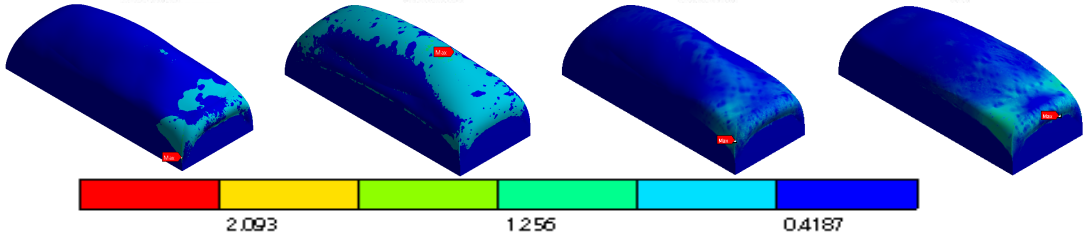			
CPO	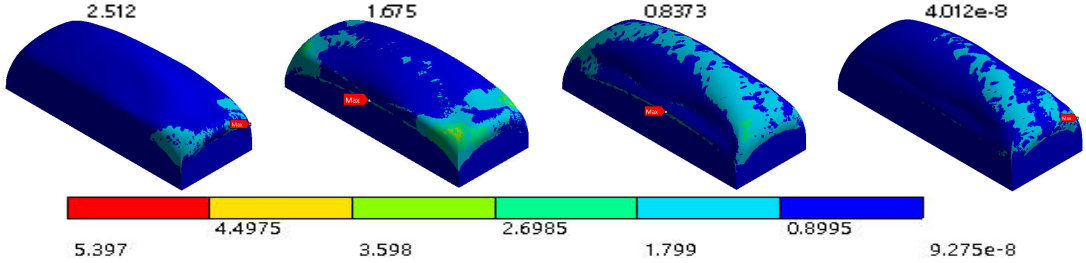			

3.4 Elastic Equivalent Strain

The elastic equivalent plastic is the total strain energy of this plastic deformation value on a material. In isotropic hardening material models, the von-mises elastic equivalent strain might be used to account for the hardening effect and determine how much permanent strain has accumulated in a structure [31].

The variation of elastic equivalent strain with different filling volume capacity is illustrated in Figure 5. The location of the line that was used to measure the strain on the Flexitank structure is shown in Figure 5(d). In comparison to other capacities, the reference capacity gives a lower value for elastic equivalent strain. According to the graph, the maximum value of elastic equivalent strain increases irregularly with increasing the filling volume capacity. As expected for all type of fluid, the maximum elastic equivalent strain occurred at the front-top of the flexitank structure. This can be convinced by referring to the contour of total deformation and von-mises stress on Table 4 and Table 5. Hence, it can be concluded that because of the hydro pressure acted on the flexitank structure, the elastic equivalent strain will be increase as the pressure increase. Since the situation of the

flexitank are in the braking condition, the highest elastic equivalent strain is occurred at the front-top of the flexitank structure.

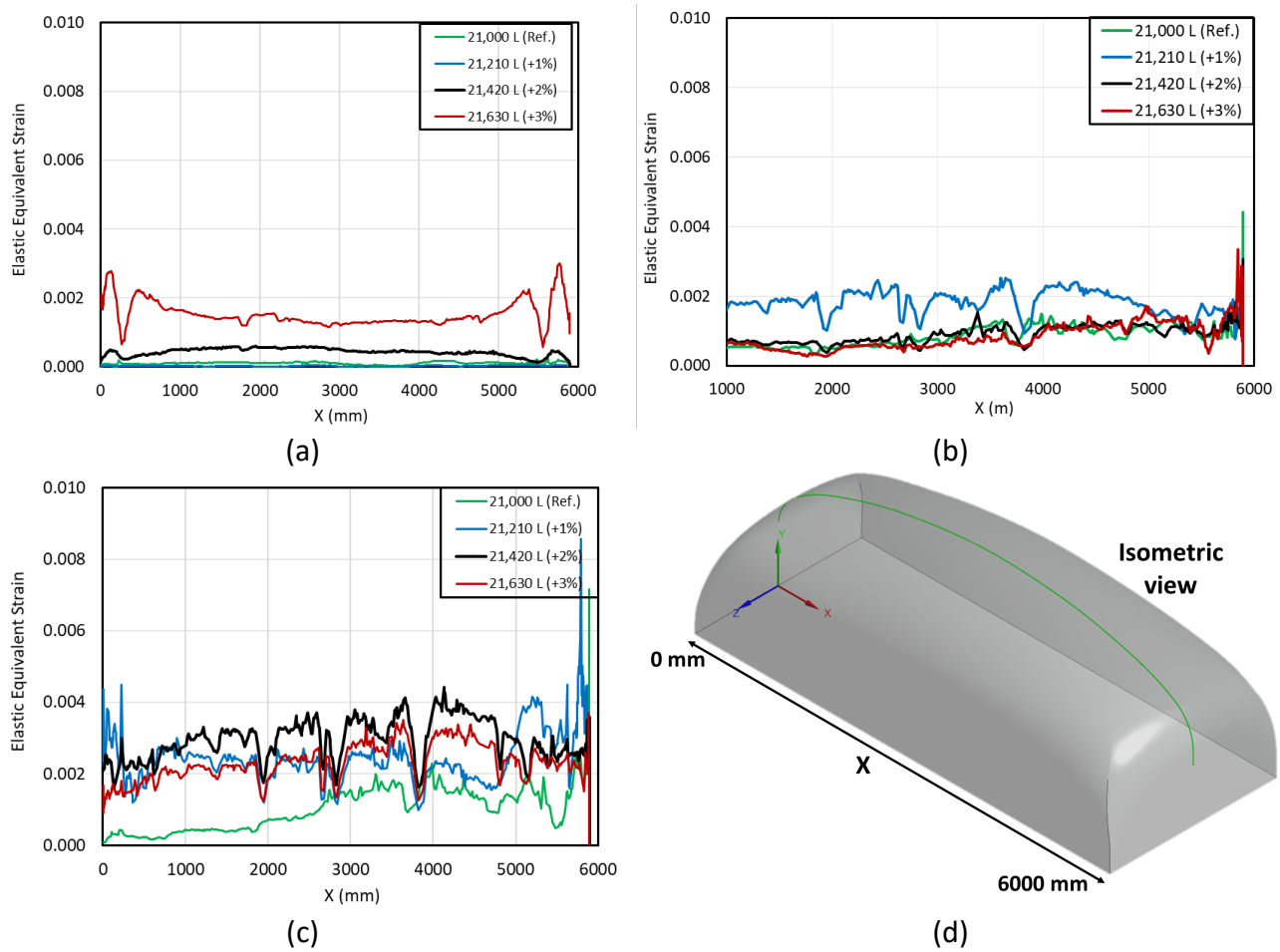

Fig. 5. Elastic equivalent strain graph in the x-direction of flexitank for (a) water (b) latex (c) CPO and (d) is the location of line used to take the value

4. Conclusion

In this study, CFD analysis was used to investigate the hydrodynamic performance on various flexitank filling volume capacity and fluid density using one-way coupling of the FSI approach. This is one of the first studies to use CFD simulation to discover the hydrodynamics effect on flexitank structure. For various filling volume capacity and fluid density, the total deformation, von-mises stress and elastic equivalent stress are presented. Increases in the flexitanks filling volume capacity, which have been investigated by analyzing the hydrodynamics impact, can lead to structural damage to the flexitanks structure. On the other hand, the total deformation and von-mises stress for reference capacity are higher than others.

Consequently, further studies should be performed, following the promising results obtained with this case, moving to more realistic structural configurations, and considering more realistic cases. Scale effects will also need to be addressed from this viewpoint.

Acknowledgement
This research was supported by Matching Grant (vot Q062) and Industrial Grant (vot M070). The author would like to thank the Faculty of Engineering Technology, Universiti Tun Hussein Onn Malaysia, and MY Flexitank Industries Sdn Bhd for providing necessary research facility for this study.

Reference

[1] Aaltonen, Alisa. "How are flexible tanks becoming a solution for wine in bulk transportation?." (2015).
[2] Kasilingam Raja, G. "Logistics and Transportation–Design and planning." (1989).
[3] Ranganathan, R., Y. Ying, and J. B. Miles. "Analysis of fluid slosh in partially filled tanks and their impact on the directional response of tank vehicles." *SAE Transactions* (1993): 505-511. https://doi.org/10.4271/932942
[4] Ng, Khai Ching, Lit Ken Tan, and Wah Yen Tey. "Meshless Fluid Structural Interaction (FSI) Simulation of Deformation of Flexible Structure due to Water Dam Break." *Journal of Advanced Research in Fluid Mechanics and Thermal Sciences*71, no. 1 (2020): 21-27. https://doi.org/10.37934/arfmts.71.1.2127
[5] Cho, J. R., and H. W. Lee. "Numerical study on liquid sloshing in baffled tank by nonlinear finite element method." *Computer methods in applied mechanics and engineering* 193, no. 23-26 (2004): 2581-2598. https://doi.org/10.1016/j.cma.2004.01.009
[6] Wu, G. X., Q. W. Ma, and R. Eatock Taylor. "Numerical simulation of sloshing waves in a 3D tank based on a finite element method." *Applied ocean research* 20, no. 6 (1998): 337-355. https://doi.org/10.1016/S0141-1187(98)00030-3
[7] Krata, Przemysław. "A method of assessment of the liquid sloshing impact on ship transverse stability." *TransNav-The International Journal on Marine Navigation and Safety of Sea Transportation* 8 (2014): 535-541. https://doi.org/10.12716/1001.08.04.07
[8] A. Veldman, "OMAE2010-20458," 2016.
[9] Godderidge, Bernhard, Stephen Turnock, Mingyi Tan, and Chris Earl. "An investigation of multiphase CFD modelling of a lateral sloshing tank." *Computers & Fluids* 38, no. 2 (2009): 183-193. https://doi.org/10.1016/j.compfluid.2007.11.007
[10] Hou, Ling, Fangcheng Li, and Chunliang Wu. "A numerical study of liquid sloshing in a two-dimensional tank under external excitations." *Journal of Marine Science and Application* 11, no. 3 (2012): 305-310. https://doi.org/10.1007/s11804-012-1137-y
[11] Vilardi, Giorgio, and Nicola Verdone. "Production of metallic iron nanoparticles in a baffled stirred tank reactor: Optimization via computational fluid dynamics simulation." *Particuology* 52 (2020): 83-96. https://doi.org/10.1016/j.partic.2019.12.005
[12] Shao, J. R., H. Q. Li, G. R. Liu, and M. B. Liu. "An improved SPH method for modeling liquid sloshing dynamics." *Computers & Structures* 100 (2012): 18-26. https://doi.org/10.1016/j.compstruc.2012.02.005
[13] Colagrossi, Andrea, Giuseppina Colicchio, Claudio Lugni, and Maurizio Brocchini. "A study of violent sloshing wave impacts using an improved SPH method." *Journal of hydraulic research*48, no. sup1 (2010): 94-104. https://doi.org/10.1080/00221686.2010.9641250
[14] Serván-Camas, Borja, J. L. Cercós-Pita, Jonathan Colom-Cobb, Julio García-Espinosa, and Antonio Souto-Iglesias. "Time domain simulation of coupled sloshing–seakeeping problems by SPH–FEM coupling." *Ocean Engineering* 123 (2016): 383-396. https://doi.org/10.1016/j.oceaneng.2016.07.003
[15] Saripilli, Jai Ram, and Debabrata Sen. "Numerical studies on effects of slosh coupling on ship motions and derived slosh loads." *Applied Ocean Research* 76 (2018): 71-87. https://doi.org/10.1016/j.apor.2018.04.009
[16] Arora, Sampann, Sudharsan Vasudevan, SRDJAN SASIC, and SASSAN ETEMAD. "A PARTITIONED FSI METHODOLOGY FOR ANALYSIS OF SLOSHING-INDUCED LOADS ON A FUEL TANK STRUCTURE."
[17] Ganuga, R. S., Harish Viswanathan, S. Sonar, and A. Awasthi. "Fluid-structure interaction modelling of internal structures in a sloshing tank subjected to resonance." *International Journal of Fluid Mechanics Research* 41, no. 2 (2014). https://doi.org/10.1615/InterJFluidMechRes.v41.i2.40
[18] "Container Owners Association Code of Practice-flexitank operators", Accessed: Jul. 14, 2022. [Online]. Available: www.containerownersassociation.org
[19] R. M. Abu Shmeis, "Water Chemistry and Microbiology," *Compr. Anal. Chem.*, 81 (2018): 1–56. https://doi.org/10.1016/bs.coac.2018.02.001
[20] "Neoprene Vs. Natural Rubber." https://sciencing.com/neoprene-vs-natural-rubber-7443733.html (accessed Jul. 14, 2022).
[21] Bahadi, Murad Awadh, Jumat Salimon, and Abd-Wali M. Japir. "The physicochemical and thermal properties of Malaysian high free fatty acid crude palm oil." In *AIP Conference Proceedings*, vol. 1784, no. 1, p. 030002. AIP

Publishing LLC, 2016. https://doi.org/10.1063/1.4966740

[22] Hynčík, Luděk, Petra Kochová, Jan Špička, Tomasz Bońkowski, Robert Cimrman, Sandra Kaňáková, Radek Kottner, and Miloslav Pašek. "Identification of the LLDPE Constitutive Material Model for Energy Absorption in Impact Applications." *Polymers* 13, no. 10 (2021): 1537. https://doi.org/10.3390/polym13101537

[23] Rocha, PA Costa, HH Barbosa Rocha, FO Moura Carneiro, ME Vieira Da Silva, and A. Valente Bueno. "k–ω SST (shear stress transport) turbulence model calibration: A case study on a small scale horizontal axis wind turbine." *Energy* 65 (2014): 412-418. https://doi.org/10.1016/j.energy.2013.11.050

[24] Clark, Nigel N., James J. Daley, Ralph D. Nine, and Christopher M. Atkinson. "Application of the New City-Suburban Heavy Vehicle Route (CSHVR) to Truck Emissions Characterization." *SAE paper* (1999): 01-1467. https://doi.org/10.4271/1999-01-1467

[25] Peric´, Milovan, and Tobias Zorn. "Simulation of sloshing loads on moving tanks." In *International Conference on Offshore Mechanics and Arctic Engineering*, vol. 41979, pp. 1017-1026. 2005. https://doi.org/10.1115/OMAE2005-67581

[26] Mahmud, K. R., M. M. Rhaman, and A. K. Al Azad. "Numerical simulation and analysis of incompressible Newtonian fluid flows using FreeFem++." *Journal of Advanced Research in Fluid Mechanics and Thermal Sciences* 26, no. 1 (2016): 1-19.

[27] Hirt, Cyril W., and Billy D. Nichols. "Volume of fluid (VOF) method for the dynamics of free boundaries." *Journal of computational physics* 39, no. 1 (1981): 201-225. https://doi.org/10.1016/0021-9991(81)90145-5

[28] Tey, Wah Yen, Yutaka Asako, Nor Azwadi Che Sidik, and Rui Zher Goh. "Governing equations in computational fluid dynamics: Derivations and a recent review." *Progress in Energy and Environment* 1 (2017): 1-19.

[29] Truesdell, Clifford, and Walter Noll. "The non-linear field theories of mechanics." In *The non-linear field theories of mechanics*, pp. 1-579. Springer, Berlin, Heidelberg, 2004. https://doi.org/10.1007/978-3-662-10388-3_1

[30] H.-C. Wu, "Continuum mechanics and plasticity," p. 684, 2005.

[31] Asgari, Mojtaba, and Mohammad Ali Kouchakzadeh. "An equivalent von Mises stress and corresponding equivalent plastic strain for elastic–plastic ordinary peridynamics." *Meccanica* 54, no. 7 (2019): 1001-1014. https://doi.org/10.1007/s11012-019-00975-8